Hybrid Axial Active Magnetic Bearing – design, modelling and prototype

Bartlomiej SIKORA, Adam Krzysztof PILAT

AGH University of Science and Technology, Faculty of Electrical Engineering,
Automatics, Computer Science and Biomedical Engineering ,
Department of Automatic Control and Robotics
Mickiewicza 30, 30-059 Krakow, Poland
bsikora@agh.edu.pl, ap@agh.edu.pl

***Abstract*—This article presents concept, design, model and prototype of an hybrid axial magnetic bearing (HAMB). The numerical model developed in COMSOL Multiphysics is presented and analyzed. The manufactured stator and rotor were tested at the laboratory-test rig.**

I. Axial Magnetic Bearings

Axial Magnetic Bearings are used in wide range of applications, where control of the axial force and stable position of the rotating machinery in z axis is required [12],[15],[16],[17],[19].

To achieve full levitation of the rotor, together with radial magnetic bearings, axial magnetic bearings must be applied to a system. Both functions, which are performed by journal and thrust bearings, may be integrated in a single magnetic bearing. Novel structures of axial magnetic bearings with permanent–magnet–bias are widely used in flywheels and aerospace systems [1],[13],[14],[18],[20],[21].

This paper is focused on design procedure of the hybrid axial magnetic bearing. Analysis were conducted, based on 2D axisymmetric model in COMSOL Multiphysics. All aspects were considered and investigated during simulation stage. Further research will be focused on preparing 3D model and its verification with experimental results.

II. Design

In the Control Laboratory of Department of Automatic Control and Robotics, Faculty of Electrical Engineering, Automatics, Computer Science and Biomedical Engineering, research into active magnetic suspension systems [5],[8],[10] are performed and different configurations of magnetic bearings are constructed [2],[3] ,[4],[9],[11].

Motivation for design of hybrid axial magnetic bearing was setup with flexible shaft and radial bearing [6]. Presented in this paper configuration assumed vertically–oriented rotor–shaft assembly. In that case, axial magnetic bearing should have ability to compensate gravitational force acting on the rotor. In proposed solution, permanent magnets were used, in order to introduce bias flux. The structure of the HAMB was constricted by dimensions and montage of the existing bearing housing.

It was assumed, that measuring path for position sensors will be prepared and magnetic circuit of the electromagnetic system will be able to center the disc. In Fig. 1 the Hybrid Axial Magnetic Bearing 3D model is presented. Proposed configuration contains two actuators, which operate in differential mode. Armature, in a form of the disc (Fig. 2), is placed inside them, with air gap set up to 500µm on each side. Ring–shaped permanent magnets, placed in both actuators and in the disc, provide bias flux.

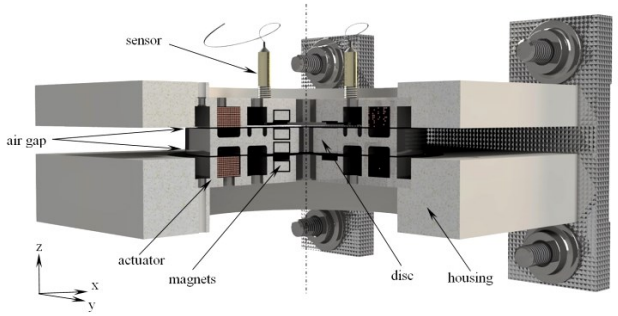

Figure 1. 3D CAD model of the Hybrid Axial Magnetic Bearing with indication of respective elements and coordinate system.

TABLE 1. NdFeB permanent magnet parameters

	Parameter	Value
D_{inner}	Inner magnet diameter	32mm
D_{outer}	Outer magnet diameter	16mm
h	Height of the magnet	3mm
L_{max}	Maximum load	8.6kg
B_r	Remanent induction	1.21T

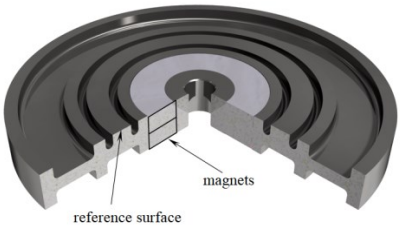

Figure 2. 3D CAD model of the disc with magnets (three–quarters view).

The designed actuator contains permanent magnet and electromagnet, which is in a form of circular coil wounded around stator (see Figure 3.). Coil consists of 125 turns of cooper wire with enameled diameter equals 0.5mm.

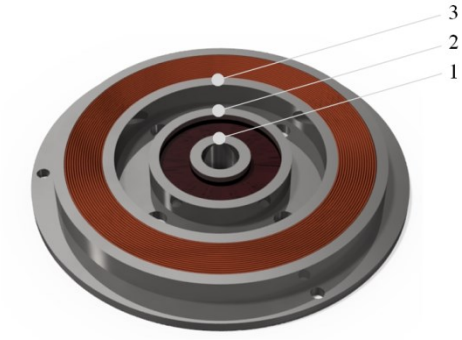

Figure 3. 3D isometric model of the HAMB actuator with selected measuring points.

III. NUMERICAL MODEL

Characteristics of the normal magnetic induction vector $B_n(z,i)$ and the electromagnetic force acting on the disc $F_{em}(z,i)$ in the function of position and current, with single HAMB actuator were provided from simulation, using finite element analysis in COMSOL Multiphysics (see Figure 4.).

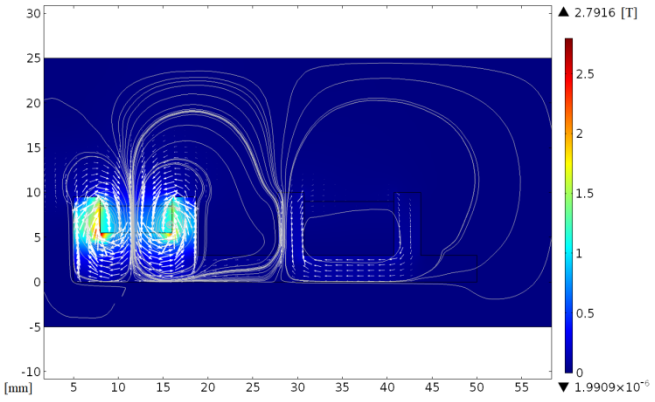

Figure 4. Magnetic induction distribution, streamlines and arrows, which point out magnetization of the permanent magnet and electromagnet in the lower actuator.

Simulation model was 2D axisymmetric, in order to reduce computational time. Meshing was extremaly fine, with maximum element size equals 0.25mm. Complete mesh consists of 90330 domain elements and 2741 boundary elements. Structural steel was chosen as a material assigned to stator and disc. Relative permeability was set up to 500. Stationary simulation with parametric sweep was performed. Firstly, single bottom actuator was simulated, in case of identification and evaluation for comparison with real experiment. Then the entire HAMB were simulated and magnetic field distribution with net force characteristic were obtained. Results are presented in what follows (Figs. 5-8).

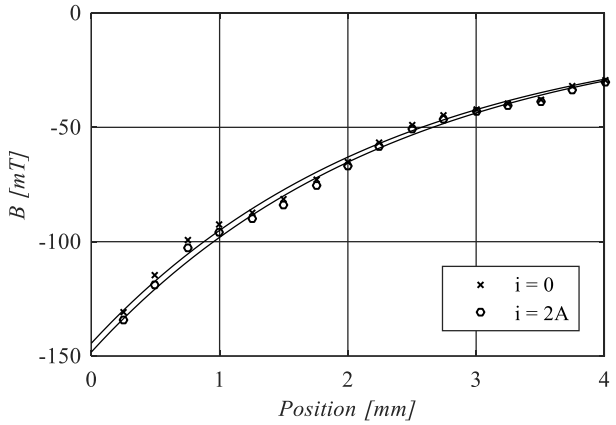

Figure 5. Magnetic induction in the function of position, for two current values and the first measuring point (see Figure 3.).

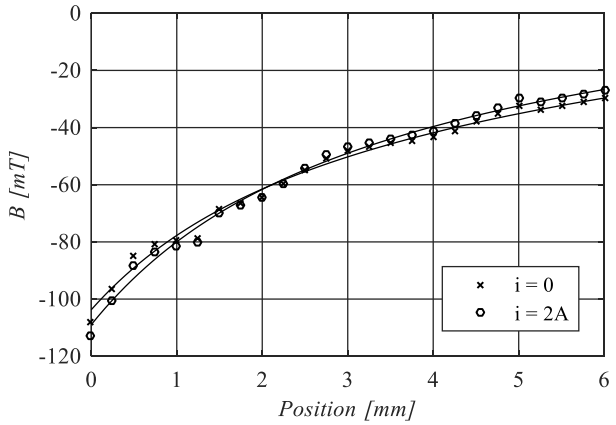

Figure 6. Magnetic induction in the function of position, for two current values and the second measuring point (see Fig. 3).

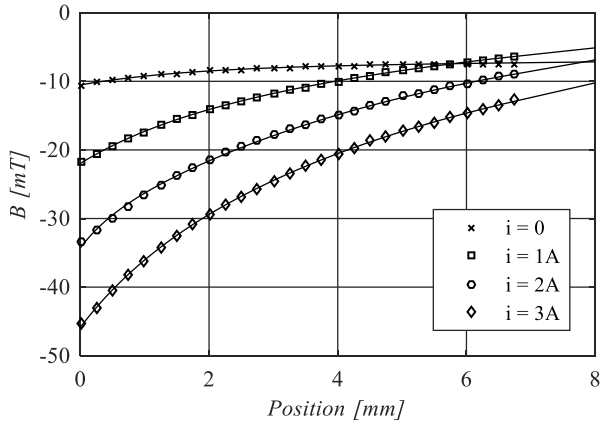

Figure 7. Magnetic induction in the function of position, for four current values and the third measuring point (see Fig. 3).

In case of 1 (Fig. 5) Figure 5. and 2 (Fig. 6) measuring point and simulation returns characteristics of magnetic induction, which are similar to each other for different current values. For a single actuator (Fig. 4) without armature, electromagnet has negligible influence on flux provided by permanent magnets. Position equals 0mm denotes surface of the armature for corresponding points depicted in Figure 3.

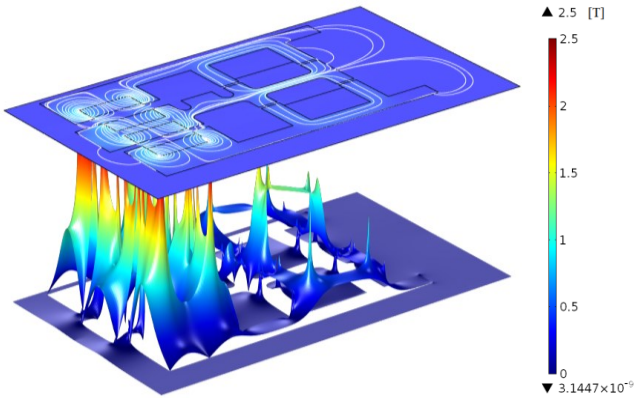

Figure 8. Height representation of the magnetic induction and its streamlines for the HAMB.

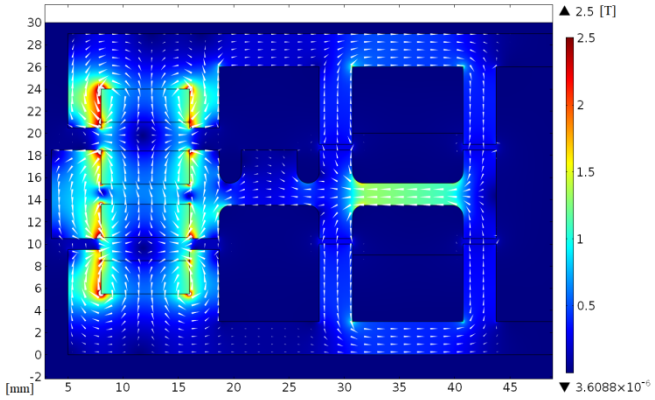

Figure 9. Magnetic induction distribution and its arrows, when the disc is located between two actuators with the same air gap on each side and with current, which drives both electromagnets, equals 2A.

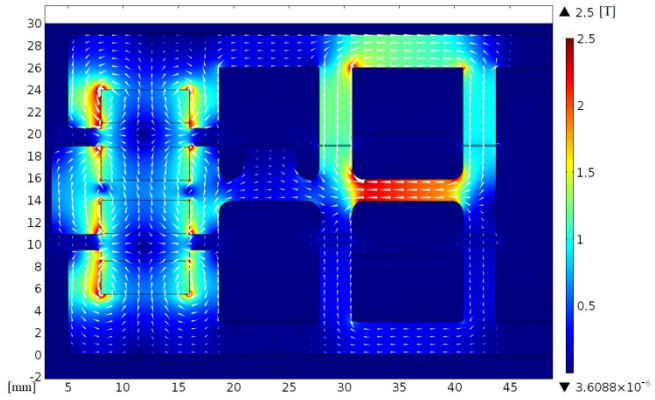

Figure 10. Magnetic induction distribution and its arrows, when the disc is almost sticked to the top electromagnet (0.1mm air gap) and with current, which drives both electromagnets, equals 2A.

Figure 11. presents net electromagnetic force acting on the disc in the HAMB. Characteristic of the force provided by permanent magnets may be approximated by linear function. For the same air gap on each side of the disc, the HAMB generates 20N force, which compensates gravitational force comming from the mass of the rotor–shaft assembly. When both electromagnets are operating in differential mode, net force adopts linear characteristic in the range from 0.3mm to 0.7 mm.

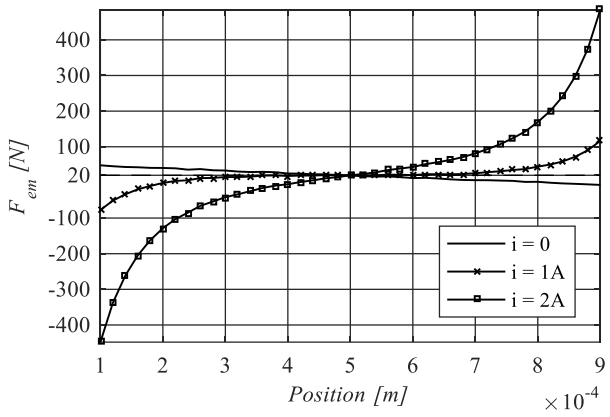

Figure 11. Net electromagnetic force acting on the disc, when both actuators operate in differential mode and are driven by the same current.

IV. Prototype

The Hybrid Axial Magnetic Bearing consists of two actuators (Fig. 12) and disc with permanent magnets (Figure 13. 13). Structural steel S355JR was used. Top and bottom actuators differ from each other height of the stator part, which surrounds permanent magnet. Such a solution enabled generation of initial force. In the top actuator 4 holes for position sensors were prepared, in order to observe behaviour of the disc. The HAMB geometry was based on the assumption, that the electromagnet could center the disc in the bearing space without introducing a radial magnetic bearing.

Figure 12. Manufactured top actuator of the HAMB.

Figure 13. Manufactured armature of the HAMB in a form of the disc.

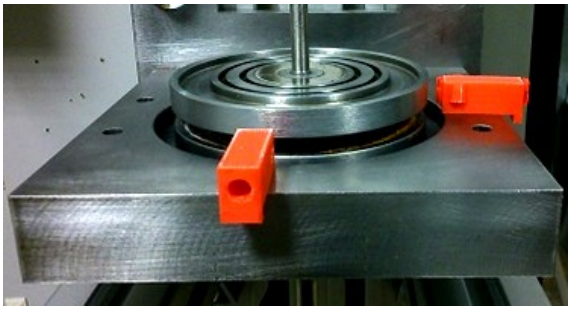

Figure 14. Disc and bottom part of the Hybrid Axial Magnetic Bearing.

The HAMB is mounted to aluminum frame from Bosch Rexrot profiles 40x40. The disc is connected with long flexible shaft via interference fit. At the end of the shaft, thin aluminum disc is attached. The other end of the shaft is free. From the top plane of the HAMB, 4 position sensors were placed, in case of precise position measurements and disc skew detection.

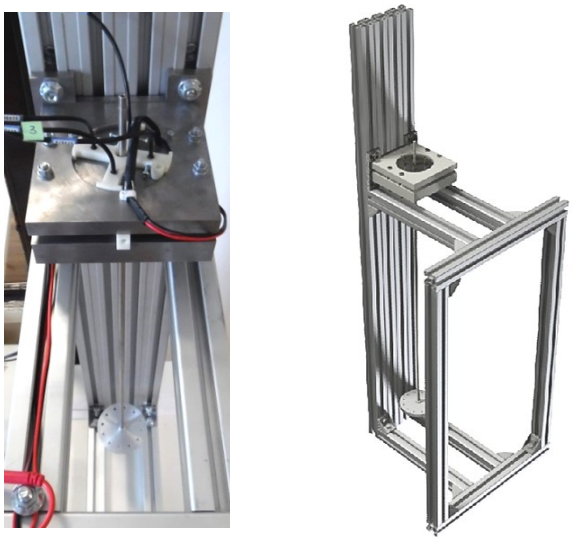

Figure 15. Laboratory test–rig with the manufactured Hybrid Axial Magnetic Bearing (left) with long flexible shaft and its 3D CAD model (right).

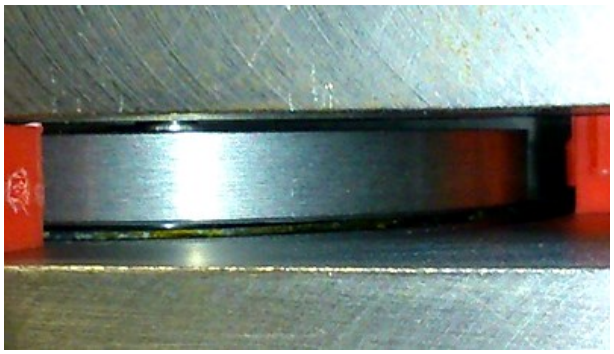

Figure 16. Completed HAMB - disc located between top and bottom actuator of the HAMB.

V. IDENTIFICATION

The magnetic induction in a function of position and current was measured, by using multifunctional hall-effect meter of magnetic field sensor SMS–102. In order to determine current characteristic, the adjustable power supply RIGOL DP832 was used, with current constraint set to 3A, maximal voltage 12V and regulated current, which feeds the winding of the electromagnet. Measurements of the magnetic induction were completed with the use of robotized setup for the magnetic field investigation [7]. Obtained characteristics show a trend comparable with simulations, however, it is visible, that magnetic field from electromagnet influences on the magnetic field around permanent magnet (see Figs. 18 and 19), which was not revealed in simulations.

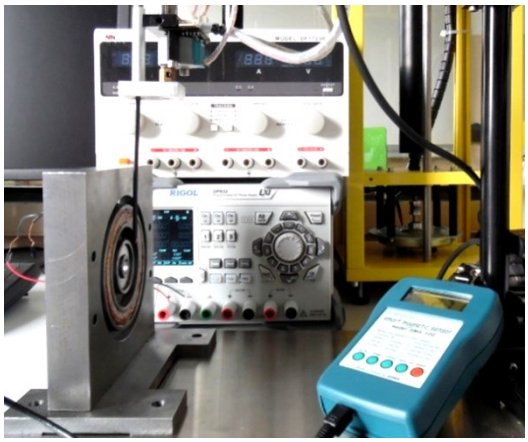

Figure 17. System for the magnetic induction measurements with robotized setup for the teslameter probe.

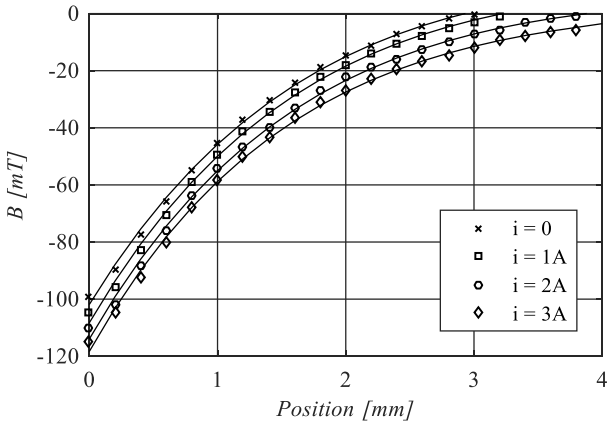

Figure 18. Magnetic induction in the function of position, for four current values and the first measuring point (see Figure 3.).

The third measuring point of the bottom actuator returns similar results from simulation (Fig. 7) and real experiment (Fig. 20). The teslameter probe has 2.4mm thickness and may introduce error resulting from measurement inaccuracy. The current characteristic is linear, without offset and with coefficient between current and voltage equals 0.3658 (see Figure 21.).

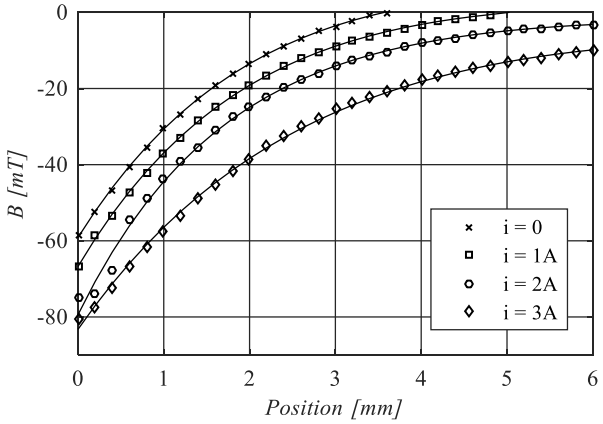

Figure 19. Magnetic induction in the function of position, for four current values and the second measuring point (see Figure 3.).

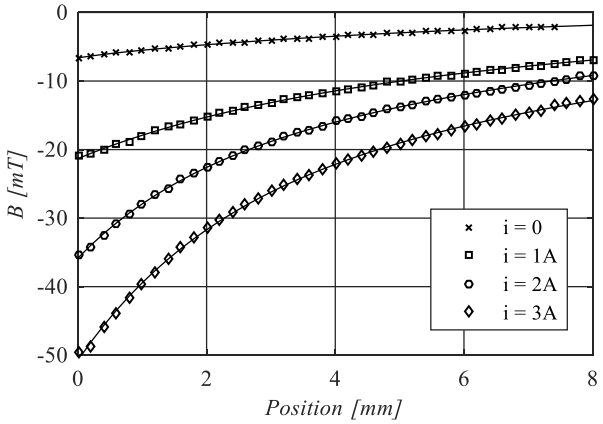

Figure 20. Magnetic induction in the function of position, for four current values and the third measuring point (see Figure 3.).

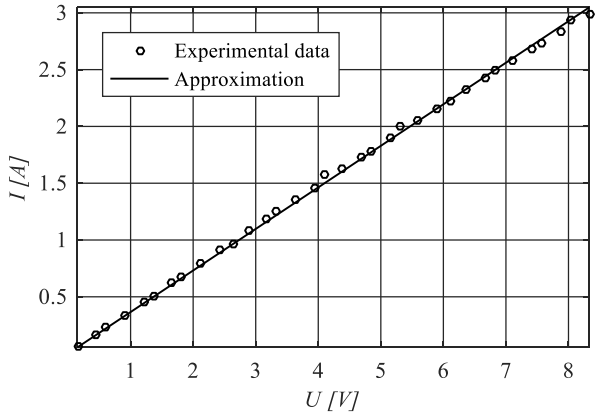

Figure 21. Current characteristic of the HAMB (bottom actuator).

VI. INITIAL LEVITATION EXPERIMENT

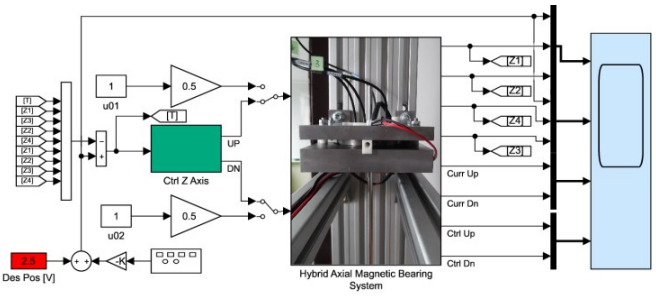

Figure 22. Data acquisition and control system of the HAMB in Simulink.

Control system is based on PID algorithm in differential mode. The error is a difference between desired and measured value of the position in V. The aim of this experiment was to check, if the operation of the electromagnet compensates the misalignment of the disc, as a result of lateral forces generated by permanent magnets. During design procedure, assumption was formulated, that the disc will be centered by the forces from electromagnets. Presented waveforms show behaviour of the disc under different conditions, but do not reflect correct operational mode of the PID control algorithm, which was tuned manually in that case.

The initial tests were realized with support of MATLAB/Simulink operating in real-time mode. The realized and tested controller can be embedded into Programmable Automation Controller [8] for the autonomous operation.

The current–mode control was implemented in the HAMB system. Such a choice deals with issues connected with slow response of the HAMB in case of voltage–mode control. An advantage of this solution is elimination of the loop-gain variation with drawback of the input voltage. In the current–driven system, control algorithm forces the current signal and the influence of the electromagnet on system response is minimized. However, if the control loop comes from the output current form inductor, noise may be introduced due to resonances from the power stage.

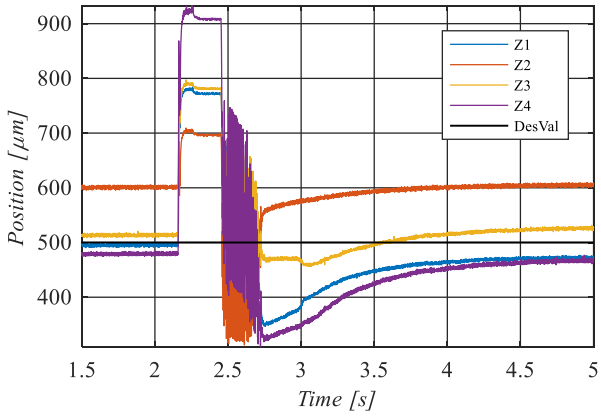

Figure 23. Position waveforms under the scenario: 1. bottom electromagnet attracted disc, 2. control algorithm was switched on.

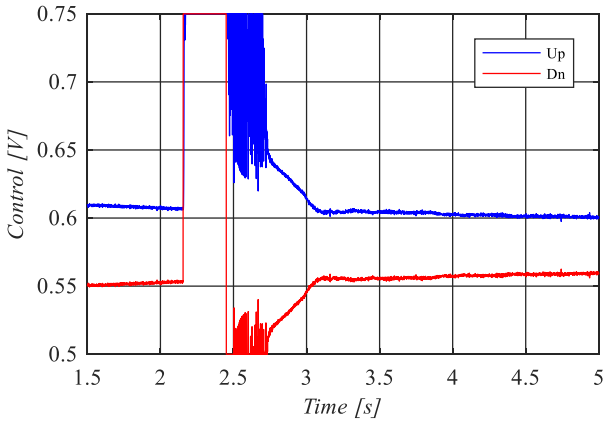

Figure 24. Control waveforms under the scenario from Figure 23.

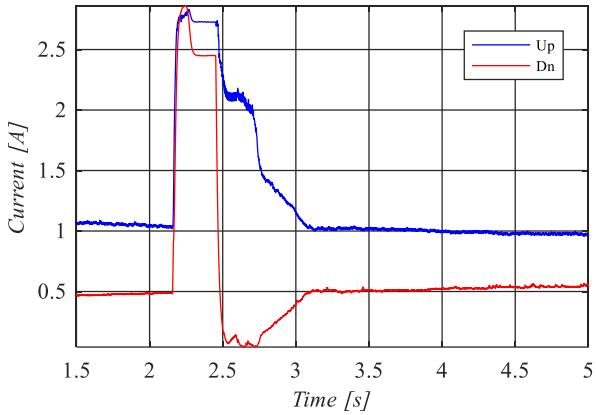

Figure 25. Current waveforms under the scenario from Figure 23.

In 2.25 [s] (see Fig. 25) disc is stocked to the bottom electromagnet and current drop may be observed, due to change of inductance, when there is no air gap between armature and actuator. When bottom electromagnet attracted the disc, the algorithm forces maximal current in top electromagnet (see Fig. 24). Afterwards, control algorithm is switched on, current from bottom electromagnet drops to 0 and top electromagnet acts on the disc.

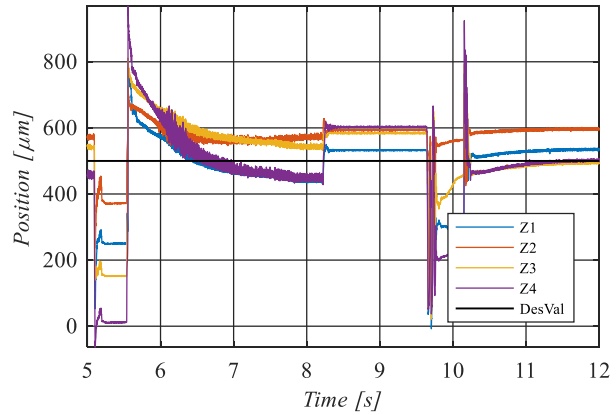

Figure 26. Position waveforms under the scenario: 1. top electromagnet attracted disc, 2. control algorithm was toogled: on – power off – power on.

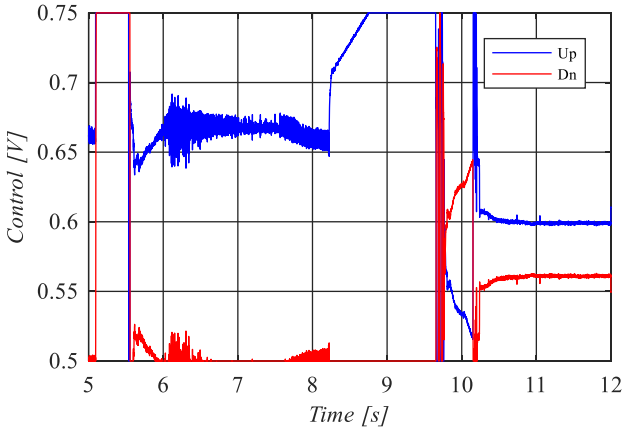

Figure 27. Control waveforms under the scenario from Figure 26.

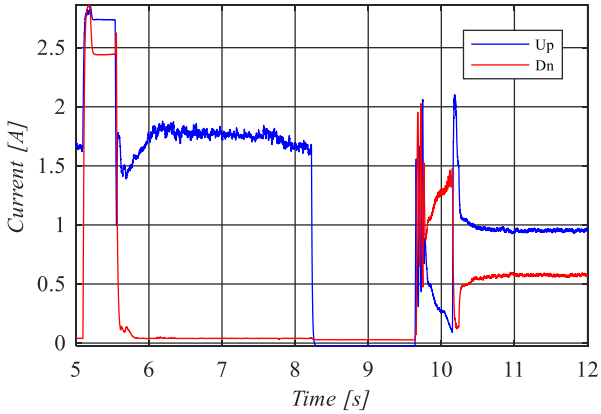

Figure 28. Current waveforms under the scenario from Figure 26.

In Fig. 26 one can find that the disc is attracted to the top electromagnet and then control algorithm is switched on. Four sensors converge to desired value – disc is skewed. Next, power supply is off – control from top electromagnet remains and both currents drop to 0 (current from bottom electromagnet is slightly bigger than 0, which may be caused by scaling error). Despite lack of power, disc levitates, lowering a bit its location. Finally, power is on and both currents reach staedy levels.

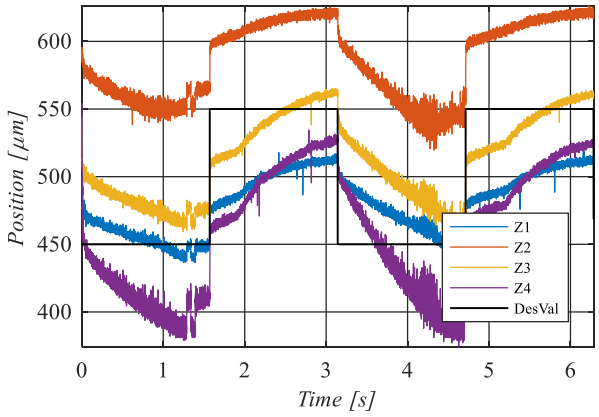

Figure 29. Position waveforms in case of square signal excitation.

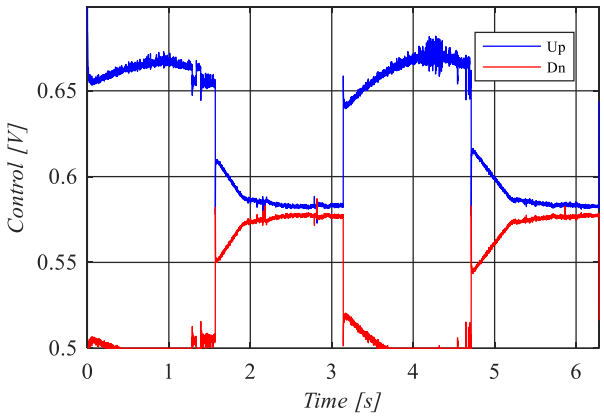

Figure 30. Control waveforms in case of square signal excitation.

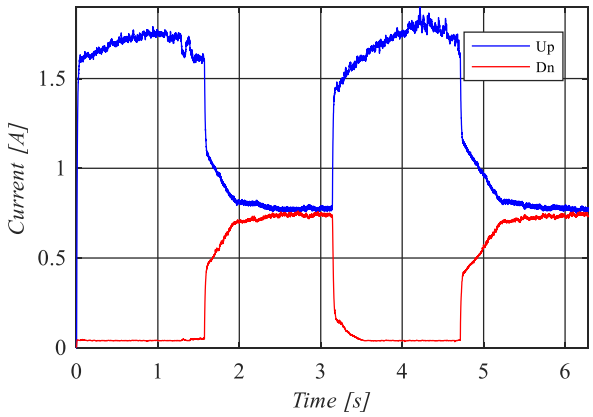

Figure 31. Current waveforms in case of square signal excitation.

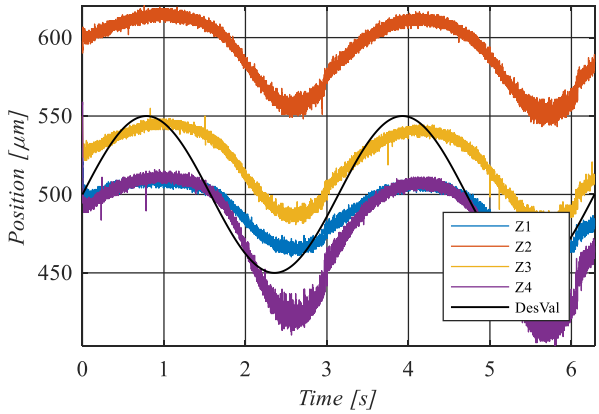

Figure 32. Position waveforms in case of sinusoidal excitation.

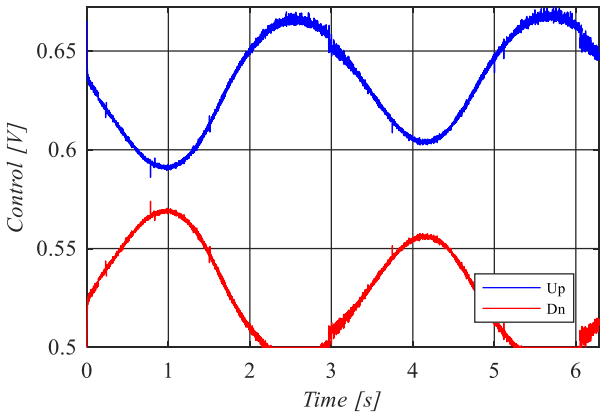

Figure 33. Control waveforms in case of sinusoidal excitation.

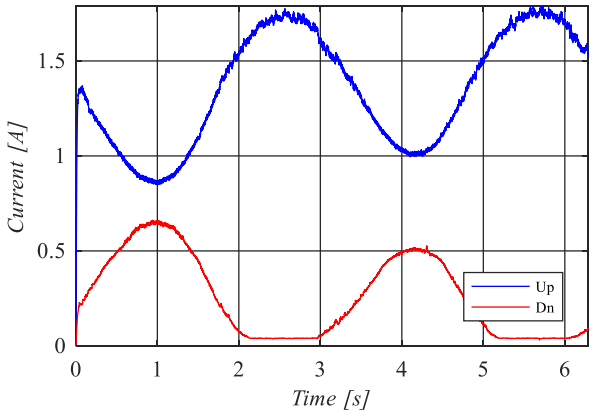

Figure 34. Current waveforms in case of sinusoidal excitation.

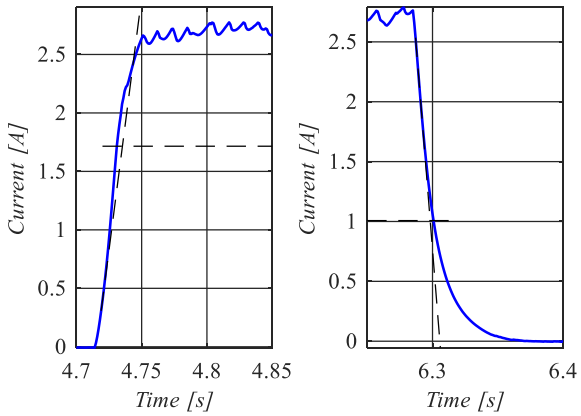

Figure 35. Time constants identification of the HAMB actuator – T_{up} = 21.2ms and T_{dn} = 13.2ms.

Figures 28-33 shows waveforms of the position, control and current for square and sinusiodal excitations. Clearly, disc is skewed and wobbles in the bearing space. In the case of sinusoidal excitation, control signal is shifted in phase to desired value.

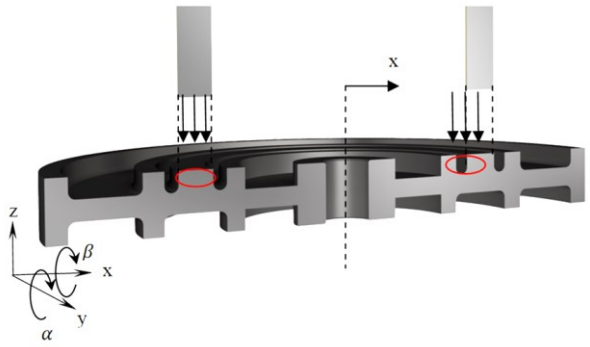

Figure 36. Scheme of sensor measurement error in case of variable disc location in the bearing space during levitation.

Measuring system consists of 4 position sensors EX–201 from KEYENCE, with sensor's head equals 5.4mm, measuring range from 0 to 1mm, analog output from 0 to 5V and frequency response up to 18kHz. Fusion of these sensors allows to obtain full observation of the disc. The reference surface (indicated in Fig. 2), which width equals 5mm, can be shifted, when disc is wobbling. This may lead to incorrect measurement. It was observed that the shaft mounted in the disk remained in contact with the chasis hole. The horizontal measurement should be added to diagnose the full levitation of the disk. Moreover, the test-rig will be extended with radial AMB.

VII. Conclusions

The Hybrid Axial Magnetic Bearing (HAMB), consisting of permanent magnets and multi-turn coils, was designed with support of the COMSOL software. The magnetic field distribution was analyzed, as well forces coming from permanent magnets and electromagnets. The magnetic flux path was adjusted respectively.

The concept with permanent magnets is applied to achieve partial load compensation of the rotor weight. The electromagnets are devoted to damping action.

The prototype of the HAMB was manufactured. The initial identification with the support of power supply and magnetic flux probe was realized. The convergence between model and prototype was accomplished. The simplification of 2D axisymmetric modelling was noted.

2D simulations did not show influence of lateral forces on the disc location in the bearing space. Differences between simulations and experiments were the result of constraints of the axisymmetric model. More accurate model, with analysis of the three–dimensional electromagnetic force vector, should be computed in 3D.

VIII. Acknowledgement

Numerical model was proceeded by using AGH Cyfronet computational resources as a part of ActRotCtrl grant. Part of this research was realized at AGH and publication was sponsored by "Incubator of Innovation +": project co-financed by the Ministry of Science and Higher Education under the program "Support for management of scientific research and commercialization of BR results in scientific units and enterprises" under the Intelligent Development Operational Program 2014-2020.

References

[1] A. Chiba, T. Fukao, O. Ichikava, M. Oshima, M. Takemoto, D. G. Dorrel, "Magnetic Bearings and Bearingless Drives", *Newnes*, 2005.

[2] A. Piłat, "An synergistic dynamic model of an active magnetic bearing with three electromagnets", in *International Symposium on Electrodynamic and Mechatronic Systems (SELM)*, pp. 23-24, Opole-Zawiercie, 2013.

[3] A. Piłat, "Analytical modeling of active magnetic bearing geometry", in *Applied Mathematical Modelling*, vol. 34, iss. 12, pp. 3805-3816, 2010.

[4] A. Piłat, "Electromagnetic Force Components Analysis in Active Magnetic Bearing numerical model", in *International Symposium on Electrodynamic and Mechatronic Systems (SELM)*, Zawiercie, 2013.

[5] A. Piłat, "Modelling, investigation, simulation, and PID current control of Active Magnetic Levitation FEM model", in *18th International Conference on Methods & Models in Automation & Robotics (MMAR)*, pp. 299-304, Miedzyzdroje, 2013.

[6] A. Piłat, "PD control strategy for 3 coils AMB", in *10 International Symposium on Magnetic Bearings*, pp. 34-39, Martigny, Switzerland, 2006.

[7] A. Piłat, "Robotized set-up for the magnetic field investigation", in *PAR Pomiary Automatyka i Robotyka*, r. 13, nr 11, pp. 18-21, 2009.

[8] A. Piłat, "Active magnetic levitation systems", Wydawnictwo AGH, Kraków, 2013.

[9] A. Piłat, B. Sikora, J. Klocek, J. Cieślik, "Laboratory test-rig of the levitating flexible rotor for unbalance control", in *International Conference Mechatronic Systems and Materials*, Zakopane, 2018.

[10] A. Piłat, W. Grega, "Reconfigurable Test-Rig for AMB Control", in *7th Conference on Active noise and vibration control methods*, Wigry, Poland, 2005.

[11] B. Sikora, A. Piłat, "Numerical Model of the Axial Magnetic Bearing with Six Cylindrical Poles", in *XLI SPETO - Conference on Fundamentals of Electrotechnics and Circuit Theory*, Ustroń, 2018.

[12] E. H. Maslen, "Magnetic Bearings", University of Virginia, Department of Mechanical, Aerospace and Nuclear Engineering, Charlottesville, Virginia, 1995.

[13] F. Jiancheng, S. Jinji, L. Hu and T. Jiqiang, "A Novel 3-DOF Axial Hybrid Magnetic Bearing," in *IEEE Transactions on Magnetics*, vol. 46, no. 12, pp. 4034-4045, Dec. 2010.

[14] F. Jiancheng, S. Jinji, X. Yanliang and W. Xi, "A New Structure for Permanent-Magnet-Biased Axial Hybrid Magnetic Bearings," in *IEEE Transactions on Magnetics*, vol. 45, no. 12, pp. 5319-5325, Dec. 2009.

[15] G. Schweitzer, "Magnetic Bearings as a component of smart rotating machinery", in *Proceedings 5th International Conference on Rotordynamics*, IFToMM, pp. 3-15.

[16] G. Schweitzer, A. Traxler, H. Bleurer, "Magnetlager", *Springer Verlag*, Heidelberg, 1993.

[17] G. Schweitzer, E. H. Maslen, H. Bleuler, M. Cole, P. Keogh, R. Larsonneur, R. Nordmann, Y. Okada, A. Traxler, "Magnetic Bearings: Theory, Design, and Application to Rotating Machinery", *Springer,* 2009.

[18] H. Lv et al., "Structure design and optimization of thrust magnetic bearing for the high-speed motor", in *IEEE International Conference on Mechatronics and Automation (ICMA)*, 2017.

[19] ISO 14839 Mechanical vibration – Vibration of rotating machinery equipped with active magnetic bearings, 2012.

[20] K. Hijikata et al., "Basic Characteristics of an Active Thrust Magnetic Bearing With a Cylindrical Rotor Core", in *IEEE Transactions on Magnetics*, 2008.

[21] T. Jiqiang, S. Jinji, F. Jiancheng, S. Ge Shuzhi, "Low eddy loss axial hybrid magnetic bearing with gimballing control ability for momentum flywheel", in *Journal of Magnetism and Magnetic Materials*, vol. 329, pp. 153-164, 2013.